Arabian Journal of Chemistry (2023) **16**, 104932

King Saud University

Arabian Journal of Chemistry

www.ksu.edu.sa
www.sciencedirect.com

ORIGINAL ARTICLE

Oxidation characteristics and thermal stability of Butylated hydroxytoluene

Suyi Dai [a], Chang Yu [b], Min Liang [a], Haijun Cheng [a], Weiguang Li [a], Fang Lai [a], Li Ma [a,*], Xiongmin Liu [a,*]

[a] *School of Chemistry and Chemical Engineering, Guangxi University, Nanning 530004, Guangxi, China*
[b] *Department of Chemistry, Hengshui University, Hengshui 053000, China*

Received 26 September 2022; accepted 22 April 2023
Available online 28 April 2023

KEYWORDS

Butylated Hydroxytoluene (BHT);
Thermal stability;
Oxidation reactivity;
Mini closed pressure vessel test (MCPVT)

Abstract Butylated hydroxytoluene (BHT) is an excellent antioxidant widely used in food, polymer materials, and other fields. In order to understand the hazards of BHT, it is necessary to study its thermal stability, oxidation properties, and reaction products. This paper investigated BHT's oxidation characteristics and products using a mini-closed pressure vessel test (MCPVT), UV radiation reaction method, iodometric method, and gas chromatography-mass spectrometry (GC–MS). The MCPVT results showed that no chemical reaction of BHT was observed under a nitrogen atmosphere even when the temperature was increased to 450 K, which indicated that it was stable. However, BHT was readily oxidized under an oxygen atmosphere with an initial oxidation temperature of 332 K. Notably, oxidation reactions can occur as low as 293 K under 365 nm UV radiations in the atmosphere. The kinetics of the initial oxidation of BHT was investigated. The kinetics of the reaction of BHT in MCPVT was a second-order reaction with the kinetic equation $\ln k = -1.2194 \times 10^4(1/T) + 21.4$. And $E_a = 101.4$ kJ mol^{-1}. The difference is that a pseudo-first-order reaction was shown under UV radiation, with a linear relationship between the apparent activation energy and the logarithm of the light intensity (I): $E_a = -1.878 \ln I + 74.56$, the apparent activation energy was significantly reduced compared to the former, indicating that UV light has a great effect on the oxidation of BHT. The peroxide value of the BHT oxidation product in MCPVT was determined with the iodometric method. When the reaction was carried out at 358 K for 8 h, the peroxide value of BHT was 3.2 mmol kg^{-1}. The main oxidation products of BHT were identified with GC–MS, such as 2, 6-di-*tert*-butyl-p-benzoquinone, 1-(2, 4, 6-trihydroxyphenyl) butanone, 3, 5-di-*tert*-butyl- 4-hydroxybenzaldehyde, 3, 5-di-*tert*-butyl-4-hydroxyacetophenone. Based on these oxidation products, the oxidation pathway of BHT was described. In conclusion, the oxidation characteristics of BHT were studied in detail with MCPVT, and a method for evaluating thermal stability was developed. UV radiation made BHT more susceptible to oxidation reactions. These data provided a reference for BHT's storage, transportation, and safety evaluation.

* Corresponding authors.
E-mail addresses: 2014401027@st.gxu.edu.cn (S. Dai), 13036819261@163.com (C. Yu), liangmin0413@163.com (M. Liang), navycheng2671@126.com (H. Cheng), lwgxqz@163.com (W. Li), laifang200609@126.com (F. Lai), gxumali@126.com (L. Ma), xmliu1@gxu.edu.cn (X. Liu).

https://doi.org/10.1016/j.arabjc.2023.104932
1878-5352

1. Introduction

Synthetic phenolic antioxidants are commonly used to reduce the adverse effects of oxygen due to their ability to trap free radicals(Liu and Mabury, 2020). Butylated hydroxytoluene (BHT) is one of the most widely used synthetic phenolic antioxidants. Due to its good antioxidant properties, ease of synthesis, and low price, it is frequently used in food, fuel, cosmetics, and other fields (Ousji and Sleno, 2020; Wang et al., 2021c; Zhao et al., 2019).

BHT has been used in increasing amounts since its development in the 1940s. The global phenolic antioxidants market is expected to grow 5% annually to reach US$18.3 billion by 2023. In China, the annual production of BHT is 9,000 tons (Wang et al., 2021b). Due to its widespread use, it is already in large quantities in the environment (Liu and Mabury, 2019; Lu et al., 2019; Zamzam et al., 2020). Humans can get additives into the body by ingesting food. The maximum allowable level of BHT in food, beverages, or oil products as defined by the U. S. Food and Drug Administration (FDA), the European Union (EU), and CODEX standards is 200 $mg{\cdot}kg^{-1}$(Sarmah et al., 2020). Nevertheless, human exposure to BHT and its metabolites is inevitable, and health concerns are alarming. BHT and its metabolites have been detected in human nails and urine. The metabolites of BHT, mainly 2,6-di-*tert*-butylcyclohexa-2,5-diene-1,4-dione (BHT-Q), 2,6-di-*tert*-butyl-4-(hydroxyethyl)phenol (BHT-OH), 3,5-di-*tert*-butyl-4-hydroxybenzoic acid (BHT-COOH), and 3,5-di-*tert*-butyl-4-hydroxybenzaldehyde (BHT-CHO), exhibit stronger toxicity than BHT (Li et al., 2019a; Wang and Kannan, 2019). BHT has been reported to be carcinogenic, and its transformation products can cause DNA damage and apoptosis. They have even been detected in pregnant women and fetuses(Achar et al., 2020; Du et al., 2019). Toxicity studies of BHT and its transformation products indicate they are a potential threat to human health.

BHT is the most common of the antioxidants added to fuels to retard the risk of explosion caused by the formation of peroxides in fuels at high temperatures. Usually, the total concentration of fuel additives ranges from 17 $mg{\cdot}L^{-1}$ to 24 $mg{\cdot}L^{-1}$(Frauscher et al., 2020). It was found that the addition of antioxidants, including BHT, to jet fuel had the effect of inhibiting oxidation. However, when jet fuel is used as an aircraft coolant, antioxidants tend to be deposited under short-term thermal effects (Jia et al., 2022). Deposition can lead to an increase in jet fuel viscosity, resulting in fouling and clogging of the aircraft, causing a hazard (Jia et al., 2021).

Although quite a lot of literature describes the use of BHT in food and fuel, little attention has been paid to the thermal properties of BHT itself. The thermal behavior of antioxidants such as BHT was studied using TG and DSC by de Jesus et al. It was found that BHT evaporated after melting and did not decompose. It exhibited different crystalline forms during melting, cooling, or reheating (de Jesus et al., 2020). Frauscher et al. used a pressure vessel to study the effect of BHT degradation products on the stability of the fuel, and this study showed as a side effect that BHT is reactive in the use of some products (Frauscher et al., 2020). The thermal stability and reactivity of BHT itself in the presence of oxygen should be addressed. Thus, this work demonstrates the temperature–pressure behavior of BHT under nitrogen and oxygen. During the transportation, processing, and addition of BHT to products for application, it is inevitable to encounter oxygen, high temperature, and sunlight environments. Hence, the oxidation of BHT under different UV light irradiation in the atmosphere was also explored. This aspect has rarely been reported in the literature.

Understanding the thermal stability and reactivity of BHT is an important scientific issue. Because once oxidized, BHT may generate toxic or unstable products that may cause unsafe reactions if added to products such as food and fuels. For this purpose, a mini-closed pressure vessel (MCPVT) was used to determine BHT's temperature–pressure behavior and obtain the temperature parameters of the various reaction stages during the oxidation process. In addition, UV light's effect on BHT oxidation was investigated. The kinetics of the oxidation reaction of BHT was calculated. GC–MS detected the oxidation products of BHT, and the possible reaction pathways of BHT were speculated. These data provide a theoretical basis for storing, transporting, and adding BHT to products for use and processing.

2. Materials and methods

2.1. Materials

Shanghai Macklin Biochemical Co., Ltd. supplied BHT (99%). Heptane (99%) was obtained from Xilong Scientific Co., Ltd. KI (99.5%), and $Na_2S_2O_3$ (99.5 %) was purchased from Aladdin Industrial Corporation, China. The N_2 and O_2 (99.99%) gases were purchased from Nanning Yunlaida Gas Co., Ltd, China.

2.2. Thermal oxidation process of BHT

Based on the Pressure Vessel Test (PVT), a test method used by the UN Specialized Committee on Hazardous Materials to assess the decomposition strength of chemically hazardous materials(Liang et al., 2022; Wang et al., 2021a), the Mini-Closed Pressure Vessel Test (MCPVT) was designed to determine the temperature and pressure changes of BHT. The specific experimental process is as follows: BHT was put into a glass test tube placed in a closed pressure vessel with a capacity of 35 mL. Oxygen and nitrogen, respectively, were fed into the reactor. Compare the stability of BHT under different gas atmospheres. The temperature was set to rise from room temperature to 449 K.

2.3. BHT peroxide analysis by iodimetry

The peroxide value calculated by the iodometric method was used as a criterion for evaluating unstable hydroperoxides produced by the early rancidity of oils and fats (Fertier et al., 2020). During the oxidation of BHT, peroxides may be generated, which are shock-sensitive and unstable. Timely determination of the peroxide value of BHT helps to understand the oxidation process of BHT. The peroxides value of BHT at different times and temperatures were measured by iodimetry. About 0.8 g of oxidation products were dissolved in aqueous starch potassium iodide and the solution turned blue. The formed peroxides were reduced by potassium iodide (Equation (1)). An equal amount of iodine was released and titrated with calibrated sodium thiosulfate until the blue color disappeared (Equation (2)). The experiment was measured 3 times in parallel, and the average value was taken. Results were calculated as millimoles per kilogram ($mmol{\cdot}kg^{-1}$) of peroxides. The formula is shown in Equation (3).

$$ROOH + 2KI + H_2O \rightarrow 2KOH + ROH + I_2 \quad (1)$$

$$2Na_2S_2O_3 + I_2 \rightarrow 2NaI + Na_2S_4O_6 \quad (2)$$

$$\text{peroxide value} = \frac{c(V_{a-}V_b)}{2m} * 1000 \quad (3)$$

Where peroxide value (mmol kg^{-1}) is the peroxide content of the oxidation products, c (mol·L^{-1}) is the concentration of sodium thiosulfate, and V_a (mL) represents the volume of sodium thiosulfate consumed by the product after the reaction. V_b (mL) is the volume of sodium thiosulfate consumed by the blank, and m (g) is the mass of the sample.

2.4. Photo-oxidation process of BHT

BHT (0.40 g) was dissolved in heptane (25 mL). Then, 20 μL of the prepared solution was dropped into the bottom of the beaker to form a solid film with an area of 8.5 cm^2 after heptane volatilization. Several solid film samples of BHT with the same concentration were placed in a thermostat, and the thermostat's temperature was adjusted so that the BHT reacted at different temperatures (293.15 K, 298.15 K, 303.15 K, and 308.15 K). The thermostat was equipped with a 365 nm UV lamp. The light intensity was varied by adjusting the distance between the UV lamp and the sample film to investigate the reaction of BHT at different UV intensities (100–500 μW·cm^{-2}). For quantitative analysis of BHT, one sample was taken out every 10 min, and the sample film was dissolved in 10 mL of heptane. The content of BHT was determined by UV–vis spectrophotometer (UV-2550, Shimadzu Instruments Co., Ltd., Japan). Each group of experiments was repeated three times to take the average value.

2.5. Analysis of oxidation products

The oxidation reaction process is generally accompanied by the generation of peroxides, which are sensitive and unstable, and decompose into many secondary oxidation products (Li et al., 2019b). GC–MS is a typical means to identify phenolic antioxidants and their transformation products (Singh et al., 2022; Wang and Kannan, 2019), and it is feasible to determine the oxidation products of BHT. The formed products were determined by GC/MS-QP2010 (Shimadzu, Japan) equipped with a Rxi-5Sil fused silica capillary column (30 m × 0.25 m m × 0.25 μm) and combined with an electron impact ionization detector (70 eV). The analytical procedure was that the temperature rose to 373 K and then rose to 513 K at a rate of 15 K min^{-1} for 3 min. The injection temperature was 553 K, the injection volume was 1.0 μL, and the split ratio was 70:1; interface temperature and ion source temperature were set to 523 and 503 K, respectively; the quadrupole mass filter with m/z of 40 ~ 500 was set in full scan mode.

3. Results and discussion

3.1. Thermal stability of BHT oxidation process

To investigate the thermal stability of the BHT oxidation reaction, experiments were performed with a self-designed MCPVT apparatus (Huang et al., 2013; Whitmore and Baker, 2001). BHT was about 1.56 g, and the initial gas pressure was 0.5 MPa. The gas was regarded as an ideal gas. The temperature rose from 302.0 K to 449.0 K at a rate of 0.8 K·min^{-1}. Experimental results of T-t (temperature vs. time), P-t (pressure vs. time), and P-T (pressure vs. temperature) are shown in Fig. 1, respectively.

Fig. 1a shows no sharp peak change in the T-t curve under either nitrogen or oxygen atmosphere, indicating no apparent exothermic reaction. The boiling point of BHT is 538 K, and its vapor pressure can be considered zero. The change of pressure in the system represents the change of pressure of nitrogen or oxygen. Observing the P-t curve (Fig. 1b), no dramatic drop in pressure occurs under the nitrogen atmosphere. It indicates that BHT was stable under a nitrogen atmosphere, and no chemical reaction occurred even when elevated to 449 K. While under the oxygen atmosphere, the pressure ($t = t_0$) dropped dramatically. t_0 implied that the initial oxidation reaction took place. However, at this point, the reaction rate was low, and the pressure drop did not keep pace with the increase in temperature. The pressure increased slightly until the reaction rate started changing at t_r. The rapid oxidation reaction stage was entered at the point ($t = t_a$) corresponding to the intersection of the tangents to the pressure rise and pressure fall curves. After t_s, the pressure dropped sharply and linearly, indicating that a stable oxidation phase had been reached.

BHT reacted in a closed vessel, and the gas inside was assumed to be ideal. No gaseous products are produced in the reaction. The situation in the kettle conforms to the formula PV = nRT. V is the container volume, 35 mL, n is the mole number of gas, R = 8.314, and P and T represent the detected pressure and temperature. The oxidation reaction of BHT is shown in Equation 4.

$$BHT + O_2 \rightarrow \text{products} \quad (4)$$

The relationship between P and T can be obtained from the T-t and P-t curves, as shown in Fig. 1c. Similarly, the pressure increases linearly with temperature under a nitrogen atmosphere, indicating that the BHT does not react during this process. Under an oxygen atmosphere, the oxidation reaction occurs when the initial oxidation temperature (T_0) is reached. During the initial oxidation reaction phase, the temperature at which the oxidation rate starts to become faster (T_r), the rapid oxidation reaction temperature (T_a), and the stable oxidation reaction temperature (T_s) are all of the interest. These temperature parameters are essential for understanding the process of the BHT oxidation reaction. The temperature parameters for different masses of BHT are listed in Table 1.

As shown in Table 1, the initial temperature of the reaction of BHT with oxygen did not differ much for different masses, and the initial oxidation temperature of BHT was about 332 K. As the mass increased, T_r, T_a, and T_s decreased, indicating that the increase in mass caused the rapid oxidation reaction to proceed earlier and BHT to be more unstable. BHT is so widely used, produced in tons, and shipped everywhere. During storage and transportation, it is very likely that oxidation will occur when large quantities of BHT are placed together in a confined space in summer. Therefore, studying the thermal instability and oxidation of BHT is particularly important.

3.2. Peroxide value of BHT oxidation

Organic peroxides are dangerous and explosive (Wu et al., 2009; Xia et al., 2022). The results of MCPVT suggest that

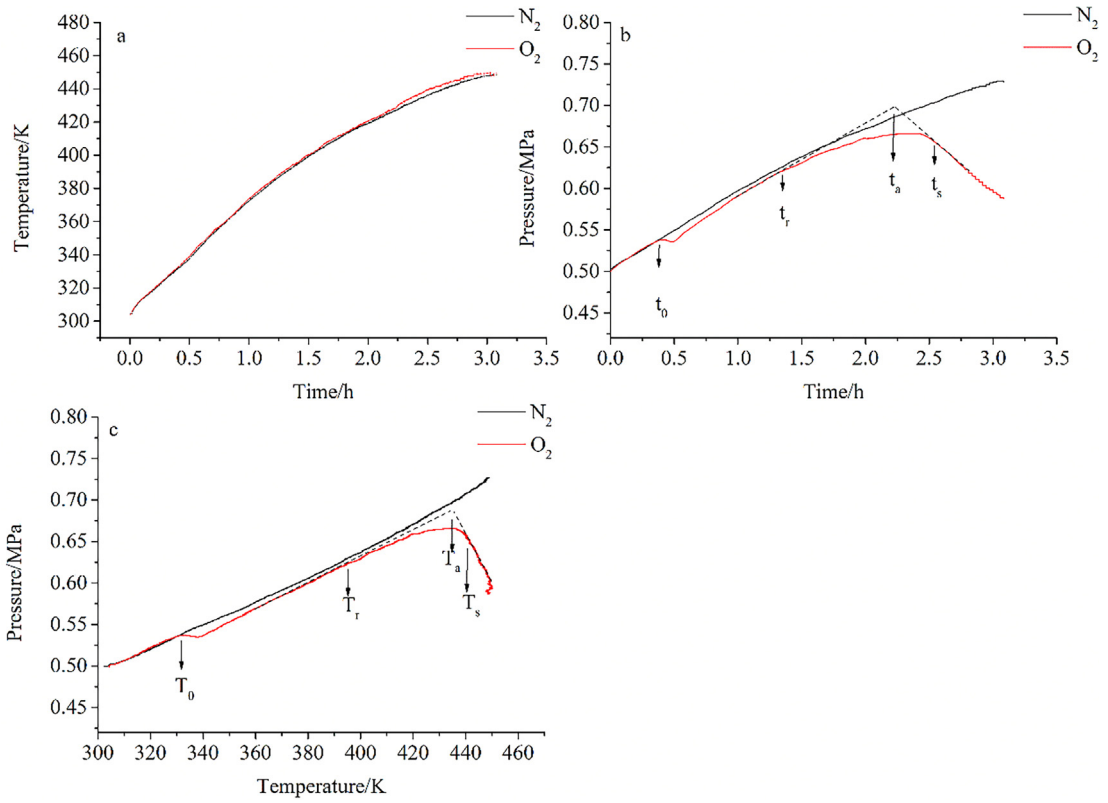

Fig. 1 Oxidation reaction behavior of BHT. (a): temperature vs. time(T-t); (b): pressure vs. time(P-t); (c): pressure vs. temperature(P-T).

Table 1 The initial oxidation (T_0), faster oxidation reaction (T_r), accelerated oxidation (T_a), and stable oxidation (T_s).

Sample/g	N_2/MPa	O_2/MPa	T_0/K	T_r/K	T_a/K	T_s/K
1.56	0.5	–	No reaction	No reaction	No reaction	No reaction
1.09	–	0.5	331.8	404.5	439.9	445.4
1.56	–	0.5	331.6	394.5	434.6	440.8
2.03	–	0.5	332.0	388.5	428.9	433.5

the oxidation reaction of BHT occurs when the oxygen pressure decreases and may produce peroxides. In some food products, it is often necessary to add some natural functional additives to improve the biological activity as well as the antioxidant capacity of the food (Rashwan et al., 2023). As a synthetic antioxidant, BHT is often used in oils and fats. (Tinello and Lante, 2020; Yang et al., 2002). The production of BHT peroxides is harmful, and it is necessary to detect the content of peroxides during the oxidation of BHT. To demonstrate the formation of peroxides, BHT was reacted at different temperatures for 8 h using MCPVT, and peroxide concentrations were measured using iodometry. The relationship between peroxide value and temperature is shown in Fig. 2.

From the results of MCPVT, the oxidation process of BHT is summarized in three steps: 1. oxygen absorption by BHT; 2. peroxide generation and decomposition; 3. deep oxidation. The results of iodometric measurements confirm the oxidation process of BHT. Fig. 2 shows that when the temperature reached T_0 (331.6 K), and the initial oxidation reaction occurred, the peroxide value increased gradually. It indicates that the oxidation of BHT occurred and peroxides gradually accumulated, at which time the generation of peroxides was faster than the decomposition. Until 358 K, the peroxide value reached a maximum of 3.2 mmol·kg^{-1}. Then, the peroxide value decreased significantly, indicating that the peroxide decomposed, and the decomposition rate was more significant than the generation rate. This is due to the fragility of the peroxide bonding energy (43 kcal·mol^{-1}), which decomposes with a slight heating or physical impact.

The MCPVT test was performed at 358 K by varying the time to observe the effect of time on peroxide generation. The relationship between the peroxide value and time is shown in Fig. 3.

As can be seen from Fig. 3, the peroxide value is time-dependent. The peroxide value increased with time, reached a maximum at 8 h, and then began to decrease. The results are in agreement with the MCPVT results. The results imply that at a specific temperature and time, BHT is known to accumulate large amounts of peroxides under an oxygen atmosphere. Organic peroxides are usually dangerous and unstable (Mohan et al., 1982). To avoid the formation of

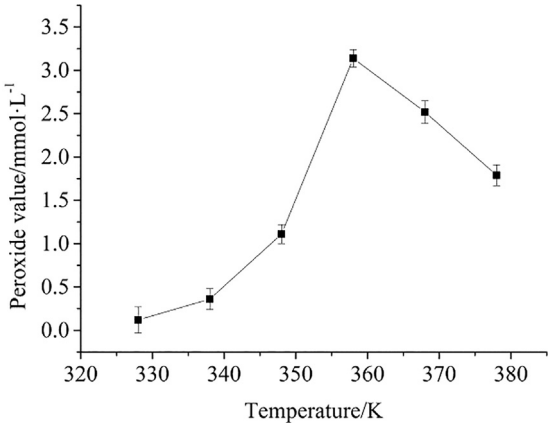

Fig. 2 Peroxide value vs. temperature.

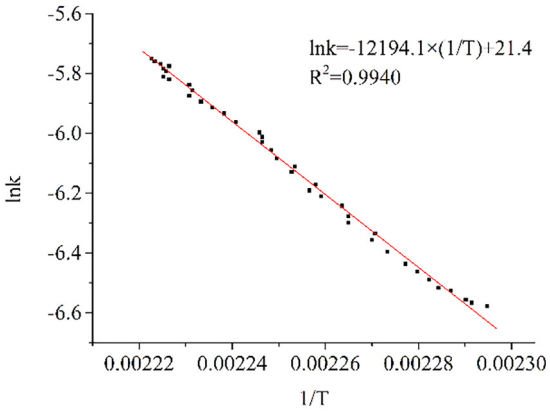

Fig. 4 Lnk versus 1/t.

BHT peroxides, the addition of oxygen should be prohibited in its production, storage, transportation, and application.

3.3. Thermo-oxidative kinetics of BHT

Chemical reaction kinetics is a crucial method for understanding the stability and reactivity of compounds. BHT is unstable under thermal, optical, and oxygen conditions, so it is necessary to learn its reaction kinetics.

Assuming that the oxygen in the kettle is an ideal gas, the mole number of oxygen can be calculated by the ideal gas equation, that is, $n_{O_2} = \frac{PV}{RT}$. P is pressure, T is temperature, V = 35 mL, and R = 8.314. In the experiment, $n_{BHT} = n_{O_2} = 0.0074mol$. According to the Arrhenius formula, a plot of lnk versus 1/T is made, as shown in Fig. 4.

There is a linear relationship between lnk and 1/T. The linear equation is as follows:

$$\ln k = -1.2194 \times 10^4 \left(\frac{1}{T}\right) + 21.4 \quad (4)$$

From the linear fitting of lnk-1/T in Fig. 4, $R^2 = 0.9940$. The apparent activation energy, $E_a = 101.4\ kJ{\cdot}mol^{-1}$, was calculated from the slope of the fitted curve. The results in section 3.1 showed that BHT did not react below 331.6 K. From 331.6 K onwards, the initial oxidation reaction occurred. In the initial oxidation phase, a rapid oxidation reaction occurred when the temperature reached 434.6 K. Above 440.8 K, a stable oxidation reaction happened. The kinetic calculations of the initial oxidation reaction show that BHT is not easily oxidized at low temperatures and that the oxidation reaction occurs after a certain amount of heat is given.

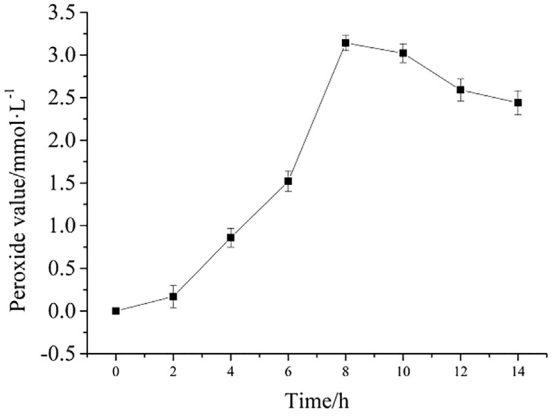

Fig. 3 Peroxide value vs. time.

3.4. Photo-oxidation characteristics of BHT

BHT may be exposed to UV light and high temperatures during transport and storage. Unlike the experiments under MCPVT, the photo-oxidation reaction was done in the atmosphere, simulating the oxidation of BHT in a realistic environment. UVA (320–400 nm) has high penetrating power. More than 95% of the long-wave ultraviolet light in sunlight can penetrate the ozone layer and clouds to reach the earth's surface (Mancuso et al., 2021). Therefore, in this paper, 365 nm UV light was chosen for the photo-oxidation of BHT. The UV absorption spectra of the BHT photo-oxidation process are shown in Fig. 5.

As seen in Fig. 5, curve (a) showed that the characteristic absorption peak of BHT was located at 283 nm. Curve (b) was the adsorption line of the photo-oxidation product of BHT. It showed that the oxide had no characteristic absorption peaks in the same range, and kinetic data can be obtained by calculating the amount of BHT.

3.5. Photo-oxidation kinetics of BHT

The photo-oxidation experiments for BHT were carried out under 365 nm UV light irradiation from 293.15 K to 308.15 K (Fig. 6) and measured every 10 min from 0 to 60 min. The light intensity (100–500 $\mu W{\cdot}cm^{-2}$) was varied by adjusting the distance between the UV lamp and the sample. During the reaction, BHT was consumed. The molarity of BHT was calculated from the standard curve of BHT ($y = 0.2083x + 0.0147$, $R^2 = 0.9999$). The consumption of BHT under different conditions was obtained.

Fig. 6 shows that BHT was consumed rapidly as the light intensity increased. The reaction rate of BHT also accelerated with increasing temperature. The data obtained at different light intensities were fitted. The fitted curves for $\ln n \sim t$ were linear, indicating that the oxidation kinetics of BHT under UV irradiation is a pseudo-first-order reaction. The reaction

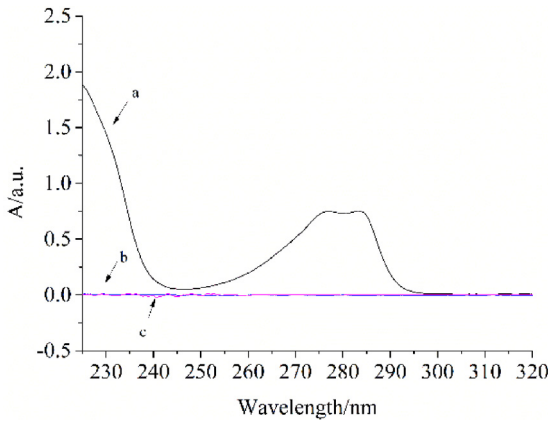

Fig. 5 UV spectra of BHT photo-oxidation process (a) BHT;(b) The UV absorption spectra of the photo-oxidant of BHT under 365 nm irradiation;(c) blank.

rate of BHT was calculated by linear fitting. E_a was also estimated from the Arrhenius equation (Equation 8). The results are presented in Table 2.

Table 2 shows that the apparent activation energy ranged from 62.50 kJ·mol^{-1} to 65.66 kJ·mol^{-1} at different light intensities. Both temperature and UV light intensity favored the reaction rate, while UV light exposure significantly affected the reaction rate. The apparent activation energy decreased with increasing light intensity, demonstrating that BHT reacted more rapidly in the presence of UV light. In addition, E_a showed an excellent linear relationship with the logarithm of light intensity. Its calculation equation is as follows:

$$E_a = -1.878\ln I + 74.56 \quad (5)$$

When MCPVT was used for thermal oxidation, the apparent activation energy was calculated to be 101.4 kJ·mol^{-1}. Under photo-oxidation conditions, the apparent activation energy decreased from 65.66 kJ·mol^{-1} to 62.50 kJ·mol^{-1} as the light intensity increased. The apparent activation energy was related to the difficulty of the reaction. A decrease in apparent activation energy indicates a more straightforward reaction.

The results show that the apparent activation energy for photo-oxidation of BHT decreases significantly in UV light, implying that BHT is more susceptible to oxidation under UV light. 365 nm of UV light is associated with natural sunlight (Kawabata et al., 2023). When using BHT products, it is vital to add a light stabilizer to prevent the exposure of BHT to UV light and high temperatures.

3.6. BHT oxidation products

The oxidation products are essential for gaining insight into the oxidation reaction's characteristics, pathways, and mechanistic inferences. In order to understand the oxidation products of BHT and explore the oxidation reaction process, GC–MS was used to detect the oxidation products of MCPVT at different temperatures for 8 h, as shown in Table 3.

Under a nitrogen atmosphere, BHT was reacted at 398 K for 8 h. The results in Table 3 show that the relative BHT content

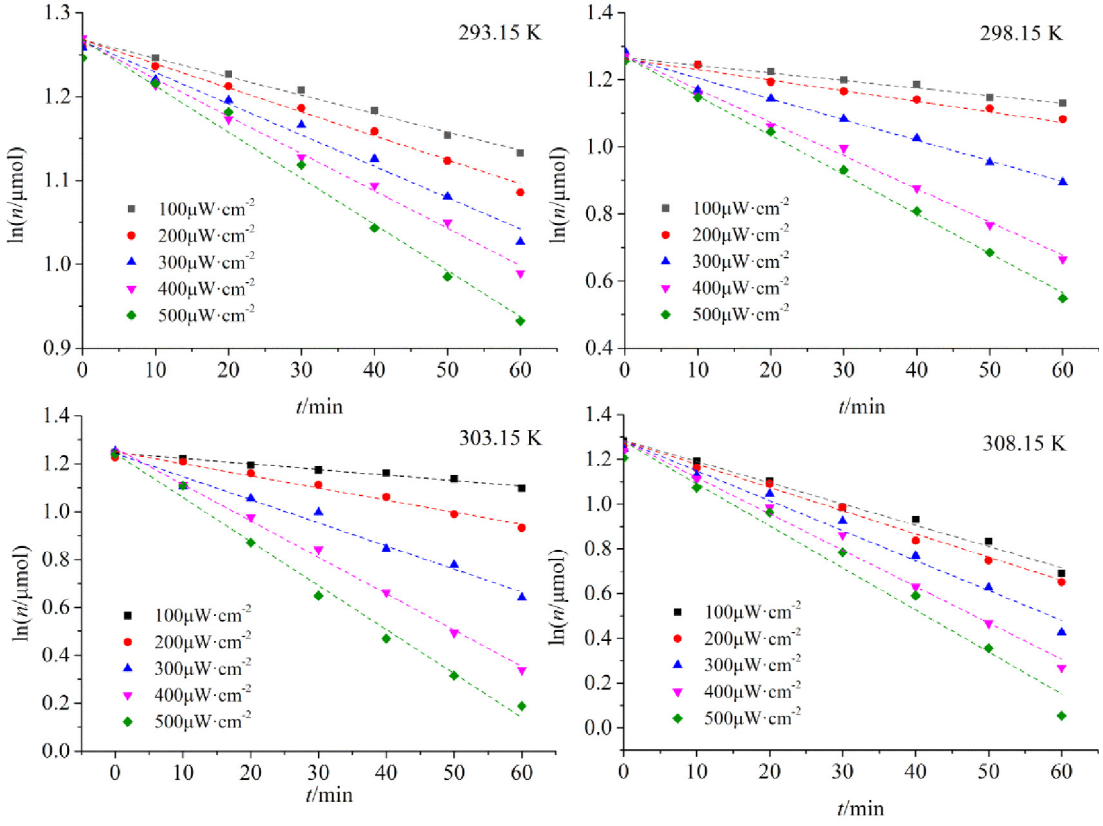

Fig. 6 Relationship between ln$n$ and t of antioxidant BHT in photo-oxidation.

Table 2 Kinetic parameters for the photo-oxidation of BHT.

I ($\mu W\ cm^{-2}$)	k(min^{-1})				E_a ($kJ \cdot mol^{-1}$)	R^2
	293.15 K	298.15 K	303.15 K	308.15 K		
100	0.0022	0.0029	0.0044	0.0085	65.66	0.9613
200	0.0029	0.0032	0.0051	0.0104	64.93	0.9591
300	0.0037	0.0062	0.0097	0.0134	64.20	0.9939
400	0.0045	0.0099	0.0152	0.0163	63.42	0.9368
500	0.0055	0.0117	0.0184	0.0188	62.50	0.9518

Table 3 Oxidation products of BHT in MCPVT.

NO.	Product	Molecular formula	Relative content (%)			
			N_2	323 K	358 K	388 K
1	2,6-Di-*tert*-butyl-p-benzoquinone (BHT-Q)	$C_{14}H_{20}O_2$	–	0.49	3.39	5.48
2	2,6-di-*tert*-butyl-4-hydroxytoluene (BHT)	$C_{15}H_{24}O$	99.2	98.13	79.69	68.93
3	1-(2,4,6-trihydroxyphenyl) butane-1-one	$C_{10}H_{12}O_4$	–	0.29	3.96	1.54
4	3,5-Di-*tert*-butyl-4-hydroxybenzaldehyde (BHT-CHO)	$C_{15}H_{22}O_2$	–	–	7.93	9.30
5	3,5-Di-*tert*-butyl-4-hydroxy acetophenone	$C_{16}H_{24}O_2$	–	–	–	3.55
6	3,5-bis(1,1-dimethylethyl)-4-hydroxy-benzoic acid	$C_{16}H_{24}O_3$	–	–	–	2.13
7	1,2-Bis(3,5-di-T-butyl-4-hydroxyphenyl) ethane	$C_{30}H_{46}O_2$	–	–	–	1.58
8	Unknown component	–	0.80	1.09	5.03	7.49

was 99.2%, indicating that BHT was stable under a nitrogen atmosphere. Under an oxygen atmosphere, BHT was oxidized at constant temperatures of 323 K, 358 K, and 388 K for 8 h, respectively. Combined with the results in section 3.2, the initial oxidation reaction stage was entered when the temperature was above 328 K, which showed a continuous increase in peroxide value. GC–MS measured the products at 323 K as 2, 6-di-*tert*-butyl-p-benzoquinone (BHT-Q) and 1-(2, 4, 6-

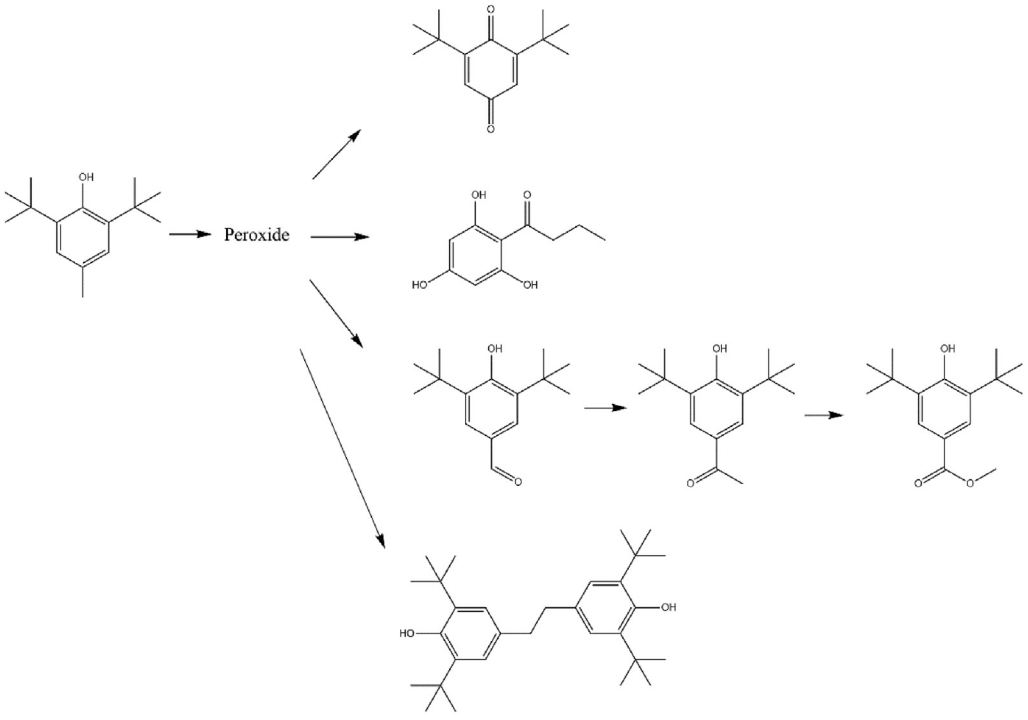

Fig. 7 Proposed pathway of BHT oxidation.

trihydroxyphenyl) butane-1-one. When the reaction temperature reached 358 K, one more product was added: 3, 5-di-*tert*-butyl-4-hydroxybenzaldehyde (BHT-CHO), and at this temperature, the peroxide value reached its highest. At 388 K, the BHT was oxidized rapidly, as the peroxide decomposition was more dominant than the generation, producing more oxidation products such as 3, 5-di-*tert*-butyl-4-hydroxyacetophenone, methyl 3, 5-di-*tert*-butyl-4-hydroxybenzoate and 3, 5-bis(1, 1-dimethyle thyl)-4-hydroxybenzoic acid. The results from the products showed that the variety of oxidation products of BHT increased at higher temperatures under an oxygen atmosphere. These include well-known metabolites such as BHT-Q, BHT-CHO, etc. BHT and its products are a potential threat to human health if used in food.

3.7. Pathway of BHT oxidation

According to the results of GC–MS, the oxidation products of BHT are complex. These oxidation products greatly help speculate the oxidation pathway and understand the oxidation process and thermal stability of BHT. The possible oxidation pathway of BHT is proposed in Fig. 7.

The oxidation reaction of BHT is complex. Combined with the results of MCPVT and iodometric measurements, the oxidation pathway of BHT was divided into three steps: 1. in the initial oxidation phase of the MCPVT test, BHT reacted with oxygen to produce peroxide; 2. the peroxide underwent decomposition and exothermic generation of many free radicals, causing a more complex oxidation reaction. 3. BHT combined through free radicals to form a dimer. The process of peroxide generation and decomposition was determined by the iodometric method. The results from GC–MS showed that the oxidation products were BHT-Q, BHT-CHO, 1-(2, 4, 6-trihydroxyphenyl) butane-1-one, 3, 5-Di-*tert*-butyl-4-hydroxy acetophenone, and 3, 5-bis (1,1-dimethylethyl)-4-hydroxy-ben zoic acid. Polymerization products are present. Under the nitrogen atmosphere, no polymerization products were found, indicating that the polymerization products result from the interconnection of free radicals generated by the decomposition of peroxides. Frauscher et al. studied the stability of the fuel using a pressure vessel and examined the products of BHT-added fuel by GC–MS. The results showed that BHT-Q and BHT-CHO were detected. It shows that when BHT is added to the fuel, the oxidation reaction of BHT occurs first, which in turn plays a role in protecting the fuel from oxidation(Frauscher et al., 2020). Studying the oxidation pathway of BHT will help BHT to be better used in different products.

4. Conclusions

The thermal oxidation process of BHT was carried out using a mini closed pressure vessel (MCPVT) to gain insight into the thermal stability and oxidation temperature of BHT. In addition, the UV oxidation reaction of BHT under the atmosphere was also investigated. The main conclusions are as follows:

1. The initial oxidation temperature parameters were measured using MCPVT, the kinetic parameters were calculated, and a method for evaluating the thermal stability was developed. The temperature and pressure behavior during the oxidation reaction was investigated by temperature–time (T-t) and pressure–time (P-t) plots. The results show that BHT is thermally stable under a nitrogen atmosphere. The difference is that the pressure of oxygen decreases significantly under an oxygen atmosphere, indicating that BHT reacts with oxygen. According to the temperature and pressure behavior, the initial oxidation reaction process is divided into four stages: initial oxidation reaction stage, accelerated oxidation reaction stage, rapid oxidation reaction stage, and stable oxidation reaction stage. The initial oxidation temperature was calculated, and initial oxidation temperature was 331.6 K. At 394.5 K, the oxidation rate started accelerating. Rapid oxidation occurred when it reached 434.6 K. Until 440.8 K, BHT entered the stable oxidation stage. That is, BHT is susceptible to oxidation under an oxygen atmosphere. The initial oxidation reaction of BHT follows the secondary reaction kinetics and the kinetic equation is $lnk = -1.2194 \times 10^4(1/T) + 21.4$, and the initial oxidation activation energy (Ea) is 101.4 kJ·mol-1. These parameters indicate the entire process of the initial oxidation reaction of BHT. It is valuable information for BHT's production, storage, transport, and application.
2. The formation of BHT peroxides was determined by the iodometric method. The highest peroxide value was obtained when the oxidation reaction continued at 358 K for 8 h.
3. The products and pathways of thermal oxidation of BHT were complex. The thermal oxidation reaction of BHT is divided into three steps: firstly, the generation of peroxides; secondly, the peroxides were decomposed, generating a large number of free radicals, which in turn triggered more complex oxidation reactions, and the oxidation products were 2,6-Di-*tert*-butyl-p-benzoquinone (BHT-Q), 1-(2,4,6-trihydroxyphenyl) butane-1-one, 3,5-Di-*tert*-butyl-4-hydroxybenzaldehyde (BHT-CHO), 3,5-Di-*tert*-butyl-4-hydroxy acetophenone and 3,5-bis(1,1-dimethylethyl)-4-hydroxy-benzoic acid; thirdly, free radicals combine to generate polymers, such as dimer of BHT.
4. The oxidation of BHT under UV radiation in the atmosphere was more significant than the thermal oxidation using MCPVT. BHT's photo-oxidation reaction followed pseudo-first-order kinetics with apparent activation energies of 62.5–65.66 kJ mol^{-1}. E_a exhibits a linear relationship with the logarithm of the light intensity: E_a= -1.878lnI + 74.56. The apparent activation energy of the BHT photo-oxidation reaction was lower than that of the thermal oxidation reaction tested by MCPVT, indicating that the oxidation reaction of BHT is more likely to occur under UV radiation.

In conclusion, this paper investigated the thermal stability, thermal oxidation reaction kinetics, photo-oxidation reaction characteristics and kinetics, and oxidation reaction products of BHT. Moreover, the peroxide concentration of the oxidation reaction was analyzed using iodometry. However, due to the low-temperature measurement sensitivity of the MCPVT device, the initial exothermic temperature obtained is not accurate, and the heat cannot be measured directly. Therefore, the MCPVT test is unsuitable for compounds with small sample mass and little heat absorption and exotherm.

CRediT authorship contribution statement

Suyi Dai: Writing – original draft, Software, Methodology, Investigation, Formal analysis, Conceptualization. **Chang Yu:** Writing – original draft, Data curation. **Min Liang:** Visualization, Supervision. **Haijun Cheng:** Supervision, Software. **Weiguang Li:** Validation, Software. **Fang Lai:** Visualization. **Li Ma:** Writing – review & editing, Supervision, Data curation, Conceptualization. **Xiongmin Liu:** Writing – review & editing, Supervision, Resources, Funding acquisition, Conceptualization.

Declaration of Competing Interest

The authors declare that they have no known competing financial interests or personal relationships that could have appeared to influence the work reported in this paper.

Acknowledgments

This work was supported by National Natural Science Foundation of China, China (21776050), National Institute of Advanced Industrial Science and Technology Fellowship of Japan, Major Science and Technology Special Project in Guangxi (AA17204087-20).

References

Achar, J.C., Nam, G., Jung, J., Klammler, H., Mohamed, M.M., 2020. Microbubble ozonation of the antioxidant butylated hydroxytoluene: degradation kinetics and toxicity reduction. Environ. Res. 186,. https://doi.org/10.1016/j.envres.2020.109496 109496.

de Jesus, J.H.F., Ferreira, A.P.G., Szilágyi, I.M., Cavalheiro, E.T.G., 2020. Thermal behavior and polymorphism of the antioxidants: BHA, BHT and TBHQ. Fuel 278, 1–11. https://doi.org/10.1016/j.fuel.2020.118298.

Du, B., Zhang, Y., Lam, J.C.W., Pan, S., Huang, Y., Chen, B., Lan, S., Li, J., Luo, D., Zeng, L., 2019. Prevalence, biotransformation, and maternal transfer of synthetic phenolic antioxidants in pregnant women from South China. Environ. Sci. Technol. 53, 13959–13969. https://doi.org/10.1021/acs.est.9b04709.

Fertier, A., Montarnal, A., Truptil, S., Bénaben, F., 2020. Jo ur na l P re Jo ur l P re. Decis. Support Syst. 113260. https://doi.org/10.1016/j.heliyon.2023.e15088.

Frauscher, M., Agocs, A., Besser, C., Rögner, A., Allmaier, G., Dörr, N., 2020. Time-Resolved quantification of phenolic antioxidants and oxidation products in a model fuel by GC-EI-MS/MS. Energy Fuels 34, 2674–2682. https://doi.org/10.1021/acs.energyfuels.9b03483.

Huang, P., Liu, X., Wada, Y., Katoh, K., Arai, M., Tamura, M., 2013. Decomposition and Raman spectrum of dimethyl ether hydrate. Fuel 105, 364–367. https://doi.org/10.1016/j.fuel.2012.06.077.

Jia, T., Zhang, X., Liu, Y., Gong, S., Deng, C., Pan, L., Zou, J.-J., 2021. A comprehensive review of the thermal oxidation stability of jet fuels. Chem. Eng. Sci. 229. https://doi.org/10.1016/j.ces.2020.116157.

Jia, T., Zhao, M., Pan, L., Deng, C., Zou, J.J., Zhang, X., 2022. Effect of phenolic antioxidants on the thermal oxidation stability of high-energy–density fuel. Chem. Eng. Sci. 247,. https://doi.org/10.1016/j.ces.2021.117056 117056.

Kawabata, K., Kohashi, M., Akimoto, S., Nishi, H., 2023. Structure determination of felodipine photoproducts in UV-irradiated medicines using ESI-LC/MS/MS. Pharmaceutics 15. https://doi.org/10.3390/pharmaceutics15020697.

Li, C., Cui, X., Chen, Y., Liao, C., Ma, L.Q., 2019a. Synthetic phenolic antioxidants and their major metabolites in human fingernail. Environ. Res. 169, 308–314. https://doi.org/10.1016/j.envres.2018.11.020.

Li, Y., Xu, X., Niu, M., Chen, J., Wen, J., Bian, H., Yu, C., Liang, M., Ma, L., Lai, F., Liu, X., 2019b. Thermal stability of abietic acid and its oxidation products. Energy and Fuels 33, 11200–11209. https://doi.org/10.1021/acs.energyfuels.9b02855.

Liang, M., Zhao, H., Dai, S., Yu, C., Cheng, H., Li, W., Lai, F., Ma, L., Liu, X., 2022. Oxidation reaction and thermal stability of 1,3-butadiene under oxygen and initiator. Arab. J. Chem. 104289. https://doi.org/10.1016/j.arabjc.2022.104289.

Liu, R., Mabury, S.A., 2019. Synthetic phenolic antioxidants and transformation products in dust from different indoor environments in Toronto. Canada. Sci. Total Environ. 672, 23–29. https://doi.org/10.1016/j.scitotenv.2019.03.495.

Liu, R., Mabury, S.A., 2020. Synthetic phenolic antioxidants: a review of environmental occurrence, fate, human exposure, and toxicity. Environ. Sci. Technol. 54, 11706–11719. https://doi.org/10.1021/acs.est.0c05077.

Lu, Z., Smyth, S.A., De Silva, A.O., 2019. Distribution and fate of synthetic phenolic antioxidants in various wastewater treatment processes in Canada. Chemosphere 219, 826–835. https://doi.org/10.1016/j.chemosphere.2018.12.068.

Mancuso, A., Cristiano, M.C., Pandolfo, R., Greco, M., Fresta, M., Paolino, D., 2021. Improvement of ferulic acid antioxidant activity by multiple emulsions. In vitro and in vivo evaluation. Nanomaterials 11, 1–16. https://doi.org/10.3390/nano11020425.

Mohan, K.V., Becker, K.R., Hay, J.E., 1982. Hazard evaluation of organic peroxides. J. Hazard. Mater. 5, 197–220. https://doi.org/10.1016/0304-3894(82)80004-6.

Ousji, O., Sleno, L., 2020. Identification of in vitro metabolites of synthetic phenolic antioxidants BHT, BHA, and TBHQ by LC-HRMS/MS. Int. J. Mol. Sci. 21, 1–13. https://doi.org/10.3390/ijms21249525.

Rashwan, A.K., Osman, A.I., Chen, W., 2023. Natural nutraceuticals for enhancing yogurt properties: a review. Environ. Chem. Lett. https://doi.org/10.1007/s10311-023-01588-0.

Sarmah, R., Kanta Bhagabati, S., Dutta, R., Nath, D., Pokhrel, H., Mudoi, L.P., Sarmah, N., Sarma, J., Ahmed, A.M., Jyoti Nath, R., Ingtipi, L., Kuotsu, K., 2020. Toxicity of a synthetic phenolic antioxidant, butyl hydroxytoluene (BHT), in vertebrate model zebrafish embryo (Danio rerio). Aquac. Res. 51, 3839–3846. https://doi.org/10.1111/are.14732.

Singh, N., Mann, B., Sharma, R., Verma, A., Panjagari, N.R., Gandhi, K., 2022. Identification of polymer additives from multilayer milk packaging materials by liquid-solid extraction coupled with GC-MS. Food Packag. Shelf Life 34,. https://doi.org/10.1016/j.fpsl.2022.100975 100975.

Tinello, F., Lante, A., 2020. Accelerated storage conditions effect on ginger- and turmeric-enriched soybean oils with comparing a synthetic antioxidant BHT. Lwt 131,. https://doi.org/10.1016/j.lwt.2020.109797 109797.

Wang, B., Huang, Y.F., Wang, P.F., Liu, X.J., Yu, C., Li, W.G., Wang, X.F., Liu, X.M., 2021a. Oxidation characteristics and explosion risk of 2, 5-dimethylfuran at low temperature. Fuel 302,. https://doi.org/10.1016/j.fuel.2021.121102 121102.

Wang, W., Kannan, K., 2019. Quantitative identification of and exposure to synthetic phenolic antioxidants, including butylated hydroxytoluene, in urine. Environ. Int. 128, 24–29. https://doi.org/10.1016/j.envint.2019.04.028.

Wang, Y.W., Li, Y.N., Lin, Q.B., Wang, X., Li, Z.H., Wu, K.X., 2021c. Functional and antioxidant properties of plastic bottle caps incorporated with BHA or BHT. Materials (Basel). 14. https://doi.org/10.3390/ma14164545.

Wang, W., Xiong, P., Zhang, H., Zhu, Q., Liao, C., 2021b. Analysis, occurrence, toxicity and environmental health risks of synthetic phenolic antioxidants: a review. Environ. Res. 201,. https://doi.org/10.1016/j.envres.2021.111531 111531.

Whitmore, M.W., Baker, G.P., 2001. A closed pressure vessel test screen for condensed-phase explosive properties in organic materials. J. Loss Prev. Process Ind. 14, 223–227. https://doi.org/10.1016/S0950-4230(00)00023-1.

Wu, S.H., Shyu, M.L., Yet-Pole, I., Chi, J.H., Shu, C.M., 2009. Evaluation of runaway reaction for dicumyl peroxide in a batch reactor by DSC and VSP2. J. Loss Prev. Process Ind. 22, 721–727. https://doi.org/10.1016/j.jlp.2008.08.004.

Xia, L., Ni, L., Pan, Y., Zhang, X., Ni, Y., 2022. Thermal Hazard Evaluation of Tert-Butyl Peroxy-3,5,5-trimethylhexanoate (TBPTMH) Mixed with Acid-Alkali. Materials (Basel). 15, 4281. https://doi.org/10.3390/ma15124281.

Yang, M., Lin, H., Choong, Y., 2002. A rapid gas chromatographic method for direct determination of BHA, BHT and TBHQ in edible oils and fats. Food Res. Int. 35, 627–633. https://doi.org/10.1016/s0963-9969(01)00164-8.

Zamzam, N.S., Rahman, M.H.A., Ghany, M.F.A., 2020. UPLC-MS/MS analysis of Sudan I, butylated-hydroxytoluene and its major metabolites from sampling sites along the Nile River-Egypt: environmentally evaluated study. Microchem. J. 153,. https://doi.org/10.1016/j.microc.2019.104432 104432.

Zhao, L., Liu, J., Zhang, X., 2019. Influencing factors of autoxidation kinetics parameters of endothermic hydrocarbon fuels. Energy and Fuels 33, 8101–8109. https://doi.org/10.1021/acs.energyfuels.9b01506.